A Geant4-based study on the origin of the sparks in a Micromegas detector and estimate of the spark probability with hadron beams

S. Procureur, J. Ball, P. Konczykowski, B. Moreno, H. Moutarde, F. Sabatié
CEA, Centre de Saclay, Irfu/SPhN, 91191 Gif sur Yvette, France
May 18, 2010

Abstract

A Geant4 simulation of a Micromegas detector in hadron beams is presented. Very large energy deposits are observed, resulting from the production of highly ionizing particles in nuclear interactions of incoming hadrons with different parts of the detector. Assuming a spark is induced by a local, large energy deposit, we find that the spark rate grows as a power law with the gain of the detector, as observed experimentally. Using measurements with alpha particles, or alternatively the well known Raether limit, our simulation gives a correct estimate of the spark rate observed in hadron beams. A few experimental tests are proposed to check the validity of this simulation.

1 Introduction

Micro pattern gaseous detectors, and in particular the Micromegas [1], play an important role in modern physics experiments. Besides their excellent spatial resolution, their fast ion collection allows them to cope with high particle rates. At very high fluxes, however, these detectors suffer from the multiplication of discharge processes, appearing when the total charge in the avalanche exceeds 10^7-10^8 electrons, the so-called Raether limit [2]. A transition to a streamer mode then occurs, leading to a breakdown in the amplification region. The resulting drop of the detector's gain therefore yields detection inefficiency, not to mention possible damage to the detector itself.

Even if extensive experimental studies have been performed to measure the spark rate with different sources (hadron beams, alpha particles) [3, 4], many aspects involved in the origin and the development of a discharge remain unclear. Before our study, the spark rate in hadron beams, as well as its dependence on the gain of the detector or on the gas mixture, could only be derived from experiments. In this paper, we present a Geant4 simulation showing that the production of Highly Ionizing Particles (HIPs) can naturally explain the observed spark rate as well as its dependence on the detector gain.

Section 2 is dedicated to the description of the Geant4 simulation of the detector. We then study in Section 3 the production of HIPs with hadron beams, and the resulting tail of the deposited energy distribution. Assuming a discharge is produced by a local, large energy deposit, we derive the spark rate in Section 4, and study the effect of the gas mixture in Section 5. Finally, we try to estimate the spark rate for a bulk Micromegas, and propose a few experimental tests to check the validity of our simulation.

2 Geant4 simulation of the detector

We simulated the Micromegas used in [3] for the first measurements of the spark rate in hadron beams, its geometry is shown in Figure 1. The detector is based on a 400 μm thick Printed Circuit Board (PCB) equipped with 7 μm thick copper readout strips. In the simulation, we did not implement the structure of the strips, but rather reweighted the density of the copper film by taking into account the width (250 μm) and the pitch (317 μm) of the strips. The 100 micron thick amplification gap is separated from the 2.45 mm drift gap by an electroformed nickel micro-mesh, 4 μm thick with 37 μm square holes every 50 μm [1]. A similar mesh has been used for the drift electrode, but with holes every 100 μm. The gas is a mixture of argon and isobutane (89-11) at atmospheric pressure, but we also tried a neon-based mixture. Finally, we did not implement the pillars maintaining the distance between the anode strips and the micro-mesh.
We used the latest version of Geant4 available at that time (4-09-02) [5], from the package developed for CLAS12 simulations, Gemc [6]. The standard physics list [2] we used is `QGSC_BERT`, one of the most reliable lists around 10-15 GeV (see Section 3.2). Systematic studies have been performed to investigate the effect of the production threshold or the integration volume for the deposited energy (Section 4.2). Because of all these systematic studies, as well as the very small probability of events we were looking for, more than 20 billion events have been generated in total.

3 HIPs production and deposited energy with hadron beams

3.1 HIPs production and origin

We first simulated the interaction of 15 GeV π^+'s in the Micromegas detector, *i.e.* at the energy used to measure the spark rate at CERN [3]. In an argon-isobutane (89-11) mixture, around 98.73% of the events contain only the incident pion which deposits an energy of the order of 1 keV that is the expected value for this particle. For 1.26% of the events, this pion creates a secondary electron in the gas volume, but this does not significantly change the deposited energy. In the remaining 0.01%, however, interactions between the pion and the material of the detector produce several secondary particles, as shown in Figure 2. We see that the production probabilities of all these particles roughly vary from 10^{-8} to 10^{-4}, indicating they can appear in large quantities at high luminosity. They usually have small momentum, as illustrated for α particles in Figure 3 (left), thus being highly ionizing. These particles are mainly produced by nuclear interactions with the drift electrode, the strips, and the micro-mesh, as shown in Figure 3 (right), the total contribution from the gas itself being relatively small. We will see, however, that if we

[1] In our simulation we actually used round holes, with the correct optical transparency.

[2] A physics list is a set of models for the various cross sections of every particle, as well as corresponding energy ranges.

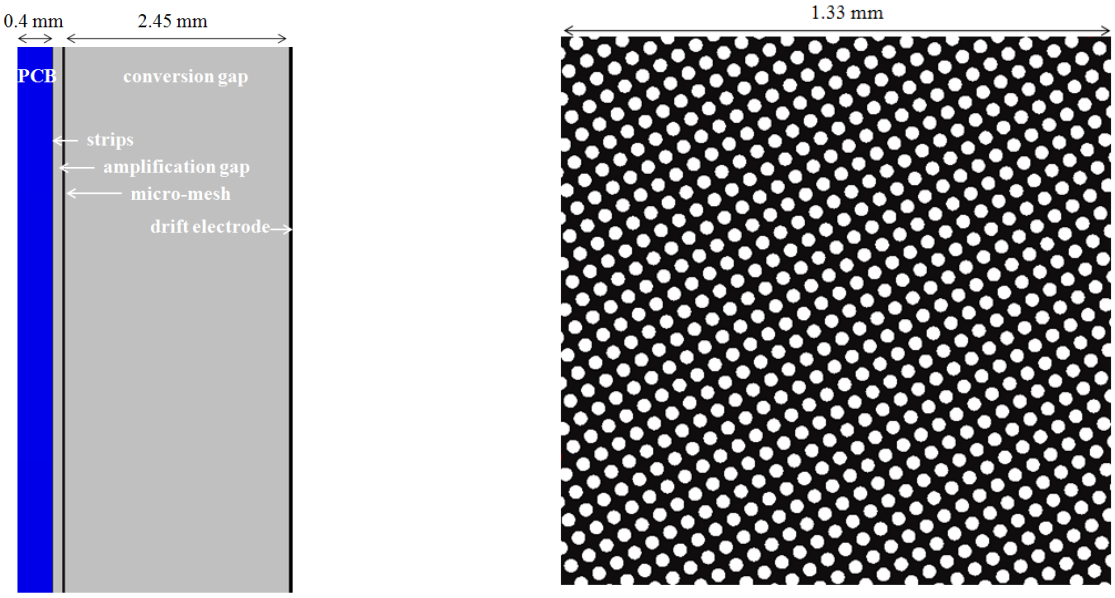

Figure 1: (Left): structure of the simulated Micromegas in Geant4. From left to right, the PCB, the strips (not visible on this picture), the amplification gap, the micro-mesh, the conversion gap and the drift electrode. (Right): structure of the micro-mesh with its holes.

only select particles with very large energy deposits, the fraction of secondaries coming from the gas is not negligible anymore.

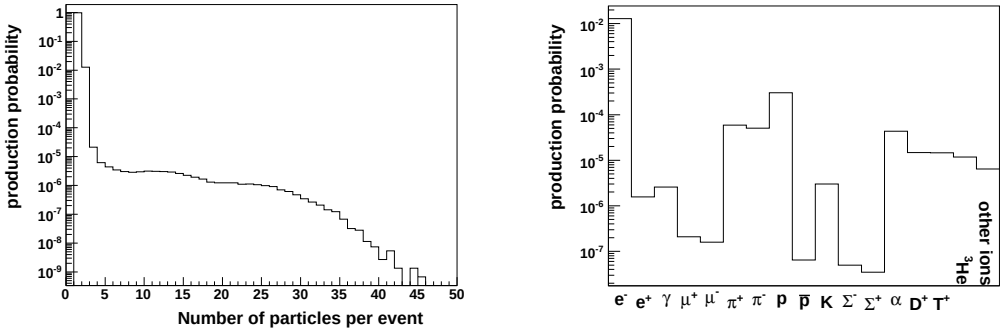

Figure 2: Left: number of particles depositing energy in the detector per event. Right: production probability for all secondary particles.

The distribution of the highest energy deposit per event in the detector is shown in Figure 4, and as expected, exhibits a very long tail coming from the HIPs. The deposited energy is integrated over fixed (track independent), square parallelograms in the detector, of size 300μm$\times 300\mu$m$\times$ the drift gap. If a particle deposits 100 keV in one parallelogram, and 120 keV in another one, only the 120 keV deposit appears in the displayed distribution.

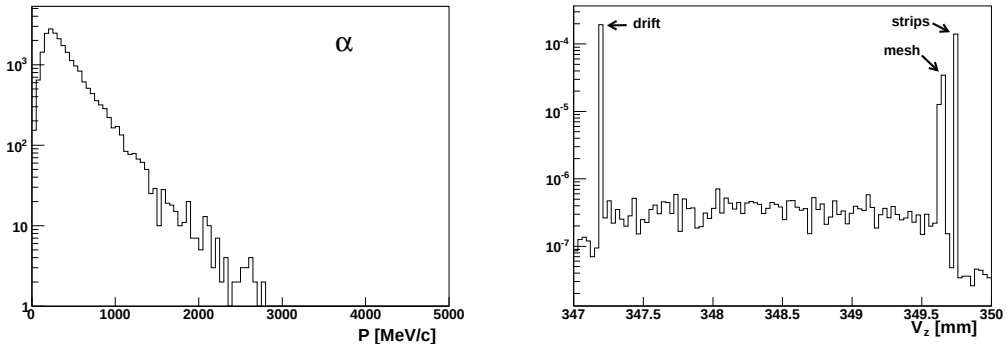

Figure 3: Left: momentum distribution for α particles. Right: vertex positions of the HIPs. The three main peaks correspond to the drift electrode, the micro-mesh and the anode strips respectively.

We see that energies of the order of 1 MeV can be locally deposited in the detector, with a probability around 10^{-8}. Around 42% of the particles depositing at least 0.2 MeV are produced in the drift electrode, 22% in the gas itself, 10% in the micro-mesh, and 23% in the strips (see also Figure 11 for comparisons with different geometries).
Figure 5 shows an example of a pion interacting with the drift electrode of the detector, producing many secondary electrons and photons, and a low energy proton.

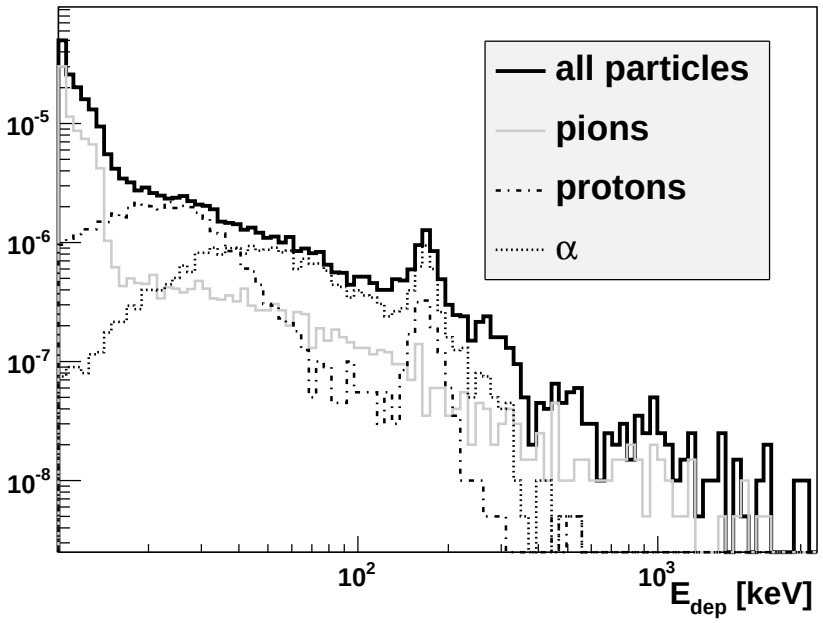

Figure 4: Tail of the local deposited energy in a Micromegas detector using a 15 GeV π^+ beam, normalized to the total flux of pions. We integrated the deposited energy over fixed parallelograms of size 300μm$\times 300\mu$m$\times$ the drift gap.

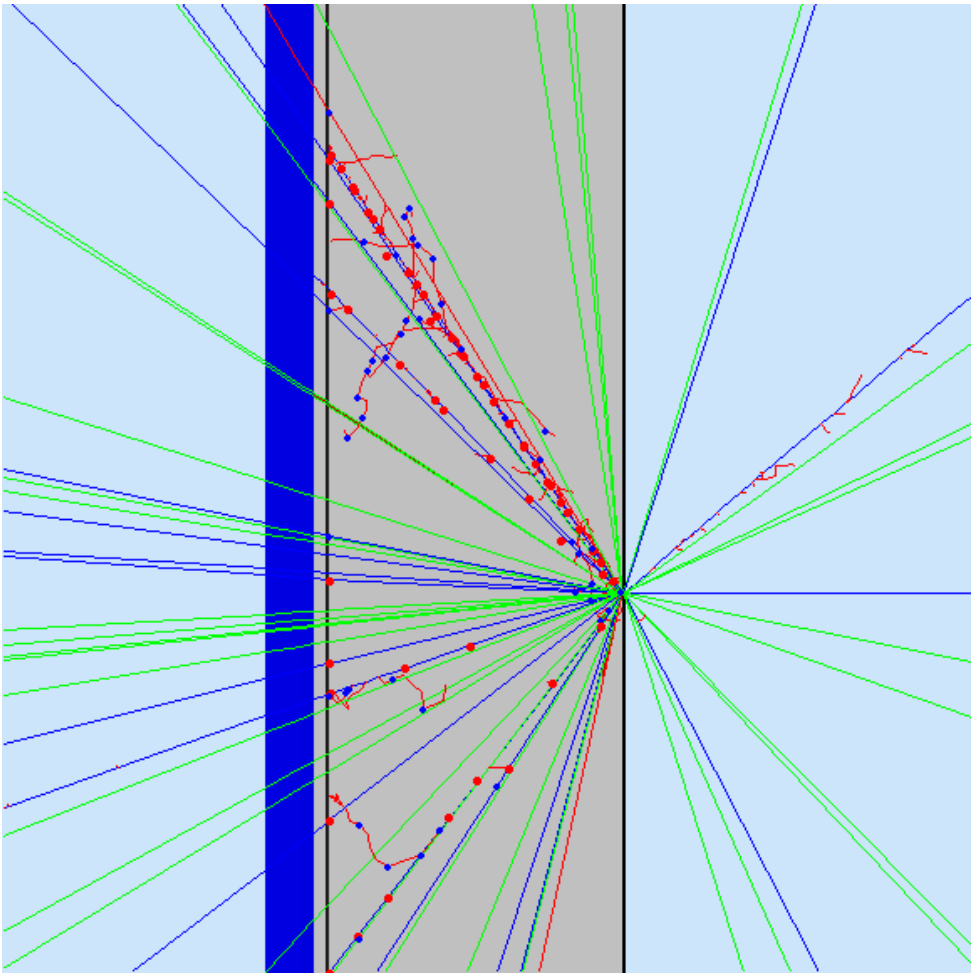

Figure 5: Example of an interaction between the incident pion (coming from the right) and the drift electrode. Besides secondary electrons and photons, a low energy proton is emitted. Large energy deposits (represented by dots) are visible all along its trajectory in the conversion gap.

3.2 Choice of the physics list and energy dependence

Before relating the tail of the deposited energy distribution with the spark rate, we need to investigate the effect of the Geant4 physics list choice. The available and recommended [7] lists are based on:

- string formation models at high energies: `QGSP` [8] (valid above 12 GeV), `QGSC` (above 8 GeV);
- cascade models at low energies: Bertini (below 10 GeV), Binary (below 1.3 to 10 GeV, depending on particles);
- parametrizations: `LEP` (valid below 55 GeV).

A Geant4 physics list often makes use of a combination of these models, to cover a large energy range. Figure 6 shows the fraction of events with large energy deposits for various physics lists, as a function of the pion beam energy. At 15 GeV this fraction can vary by an order of magnitude due to large discrepancies in secondary particle cross sections between the various physics lists. These large discrepancies come from a lack of data at these energies, however pion production on Copper at 12 GeV - *i.e.* very close to our simulation - clearly favours the `QGSC` model which is able to reproduce both the cross section and the momentum distribution of the secondary pions [9]. In the following, we will therefore use the `QGSC_BERT` physics list, the Bertini part beeing almost useless at our energies. Note that the spark rate does not exhibit a strong experimental dependence with the beam energy in the range 3-15 GeV [3]. Anticipating the correlation between large energy deposits and sparks, this observation supports our choice of the physics list, as `QGSC_BERT` indeed exhibits the smallest variation at these energies.

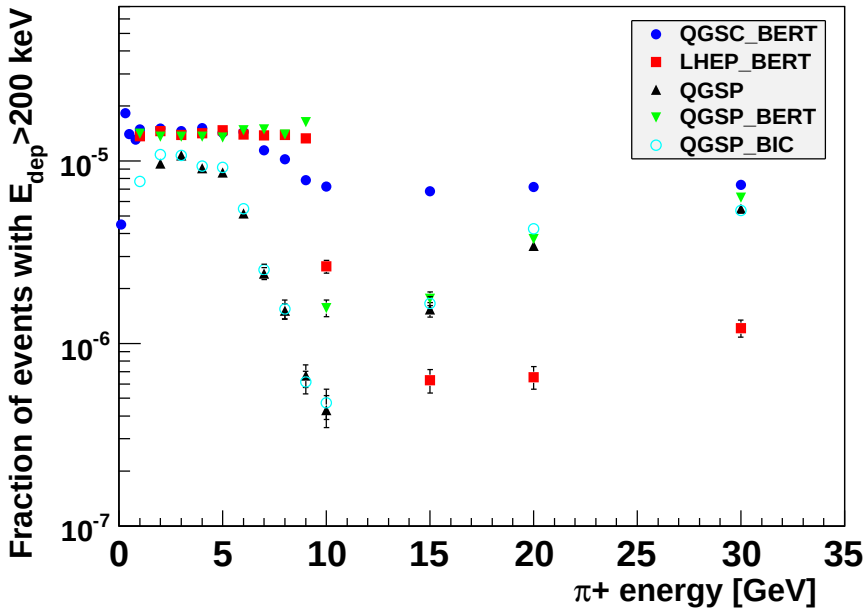

Figure 6: Fraction of events with large energy deposits for different Geant4 physics lists, as a function of the incident pion energy.

4 Spark rate

4.1 Estimation of the spark rate as a function of a normalized gain

As already mentionned, the spark rate evolution with the average gain has been studied experimentally [3], and turned out to exhibit a power law dependence. This dependence cannot be explained simply by the gain fluctuations. Indeed, the gain is known to follow a Polya law [10], and the integration of the corresponding distribution's tail cannot lead to a power law shape. It is therefore natural to assume that the sparks are due to large energy deposits in a small volume of the detector, generating a large number of electrons in the conversion gap, and leading to a spark once multiplied in the amplification gap. Assuming the number of electrons created in the conversion gap is directly proportional to the deposited energy, we can then derive the spark rate evolution with a normalized, average gain of the detector: if a deposited energy of 1 MeV creates a spark at a gain equal to unity (normalization), then a 500 keV deposit will produce a spark at a gain of 2. The normalized gain G_n needed to create a spark can then be expressed as:

$$G_n(E_{dep}) = \frac{1\ MeV}{E_{dep}}, \tag{1}$$

where E_{dep} is in MeV. Thus, the integration of the tail of the deposited energy will directly give the spark rate S at a given gain G_n:

$$S(G_n(E_{dep})) = \int_{E_{dep}}^{\infty} f(X)dX, \tag{2}$$

where f is the deposited energy distribution. The result is shown in Figure 7, where a power law dependence is clearly observed, that is qualitatively compatible with the experiments.

4.2 Effect of the Geant4 production threshold and the integration volume

The amplitude of the spark rate shown in Figure 7 may depend on two important parameters:

- the production threshold: this determines the minimum energy at which Geant4 stops to propagate the primary particles. When this minimum is reached, no additional secondaries are produced, and the primary is continuously tracked down to zero energy. To take into account differences of material, this threshold is actually a distance in Geant4. In our simulation, we set it to 300μm that corresponds to a minimum proton momentum of about 40 MeV/c in argon gas;

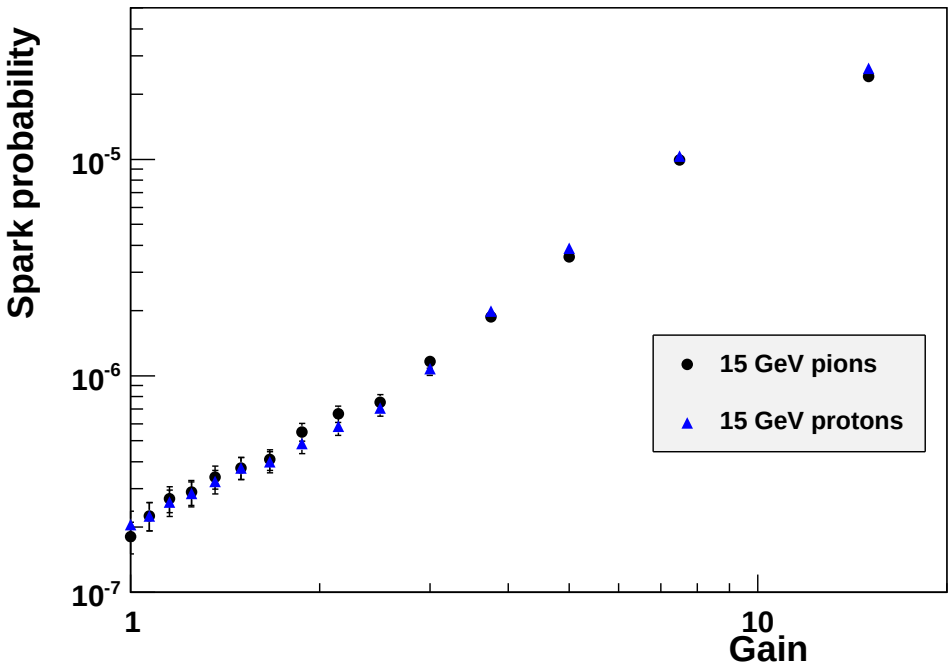

Figure 7: Simulated spark rate with 15 GeV pions and protons obtained by integrating the long tail of deposited energy, as a function of a normalized gain (see the text for details).

- the integration volume for the deposited energy: as mentionned previously, we integrated the deposited energy in boxes of size 300μm$\times 300\mu$m$\times$ the drift gap. The transverse size of these boxes should somehow reflect the transverse size of a spark: it would make no sense, for example, to integrate the deposited energy within 1 mm^2, as a spark is a much more local phenomenon, usually involving only one strip. On the other hand, as we do not simulate the transverse diffusion of electrons in the gas, it would be meaningless to integrate over sizes much smaller than this transverse spread.

Figure 8 shows the effect of these two parameters on the spark rate: no significant dependence is observed on the production threshold (the spread at small gain is due to statistics), but as expected, the spark rate increases significantly when we integrate the deposited energy over larger boxes. However, for small enough boxes, the spark rate does not vary a lot, supporting the idea that large energy deposits are very local, as it should be for HIPs stopped in the gas.
In the following, we will use the same value for the production threshold and the integration volume, *i.e.* 300 μm.

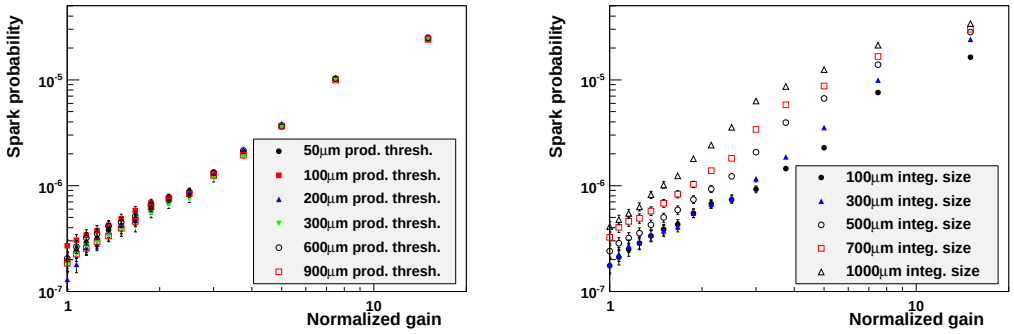

Figure 8: Left: spark rate evolution with the normalized gain, for different Geant4 production thresholds. Right: same, with different integration volumes.

4.3 Comparison with experimental data

The next step is to make a quantitative comparison between the observed spark rate and the simulated one. Therefore, we need to relate our normalized gain to a realistic one. There are essentially two ways to do it:

- by using the Raether limit, indicating that a spark appears when the total number of electron exceeds 2×10^7; however this limit is a very rough approximation, the spark probability being a smooth function of the total charge (see for example [4]);
- by using the measured spark rate yielded by a ^{241}Am source (producing α particles at 5.5 MeV). This spark rate is close to an Erf function of the gain, as expected from the nearly Gaussian amplitude distribution of the α's. As we know precisely what is the mean deposited energy for these particles, the corresponding gain - *i.e.* needed to produce a spark for this deposited energy - is simply the gain for which the spark probability is 0.5. According to measurements from [4] (Figure 4), performed with a detector identical to [3], this gain is around 2500. The mean energy deposit of α particles in this detector being around 400 keV, a gain of 1000 is required to spark with a 1 MeV deposit.

The result of these normalizations is shown in Figure 9, and are compared with experimental measurements of the spark rate. Taking into account the uncertainties from the nuclear interactions at these energies, our estimate of the spark rate is in reasonable agreement with the data.

5 Effect of the gas mixture

Another important experimental observation is the strong dependence of the spark rate on the used gas mixture [3]. Detectors used with light gases are indeed known to get less sparks than with heavy ones. The fact that only a small fraction of HIPs are created in

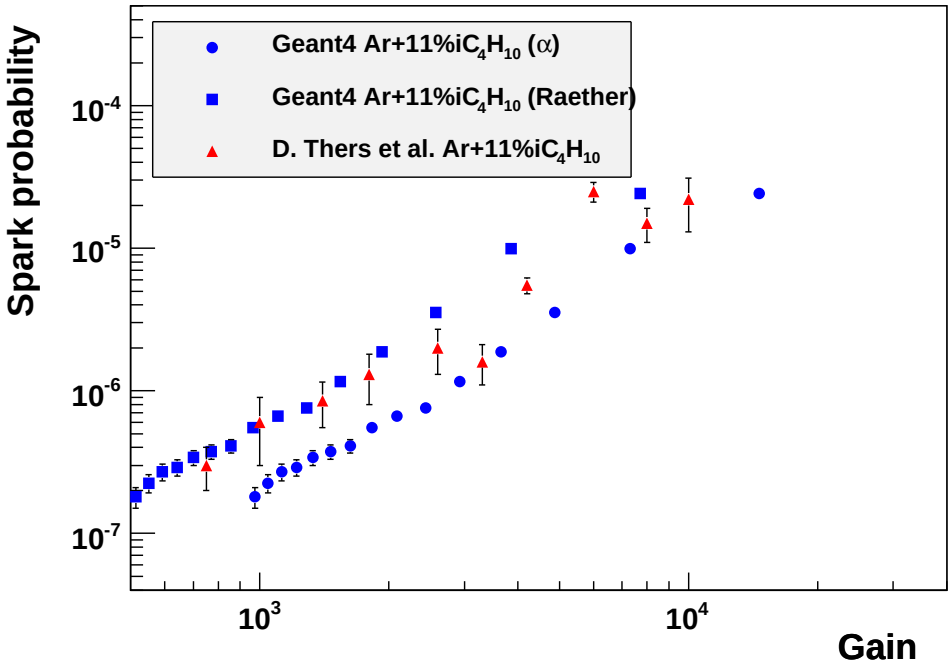

Figure 9: Comparison between simulated and measured spark rate with 15 GeV pion beam, using the two proposed normalizations for the gain. Data are extracted from the Figure 8 in [3].

the gas is not incompatible with this observation, as the gas will also play a role in the way these particles deposit their energy: in lighter gas, the mean free path is longer, and will lead to a spread of the charge, as well as to a decrease of the local electron density. But before comparing the spark rates with different gases, we need to address two issues:

- the mean energy required to create one electron-ion pair (w_i) depends on the gas: for example, it is around 36.3 eV in neon, and only 26 eV in argon. So, if a 1 MeV deposit can induce a spark in argon gas (by producing around 1 MeV/ 26 eV = 38,500 electrons) at a given gain, the same deposit in neon will produce 1 MeV / 36.3 eV = 27,500 electrons, meaning it will produce a spark only with a gain (36.3 / 26) times larger;

- this *gas gain normalization* actually assumes that the spark is induced by the same density of electrons in the amplification region, whatever the gas is. This is probably not the case in general, as gas have different dielectric strengths. However, it turns out that this dielectric strength is roughly the same for argon and neon [11]. In the following, we will therefore only compare argon and neon mixtures, assuming the spark is induced by the same electron density in both cases. This is supported by the observation that detectors spark when the Raether limit is reached, a limit that

is almost independent of the choice of gas (argon or neon).

Figure 10 shows the spark rate for argon and neon-based mixtures, with the gain normalized as in Section 4.3, and reweighted by the w_i ratios. Neon mixtures are found to have a spark probability that is significantly smaller than argon mixtures. However, the difference between argon and neon in the experimental data is even larger, and it is likely that intrinsic properties of the gas that are not taken into account in this simulation, such as the spread of the charge through the transverse diffusion or the drift velocity, do affect the spark probability. Figure 11 summarizes the contributions of the different parts of the detector to energy deposits larger than 200 keV. We see that the use of a neon mixture lowers each contribution by almost a factor of two. These simulations thus seem to indicate that the strong effect of the gas on the spark rate is not due to nuclear interactions with the gas itself, but rather to stopping power differences (and a higher ionization energy w_i for neon gas).

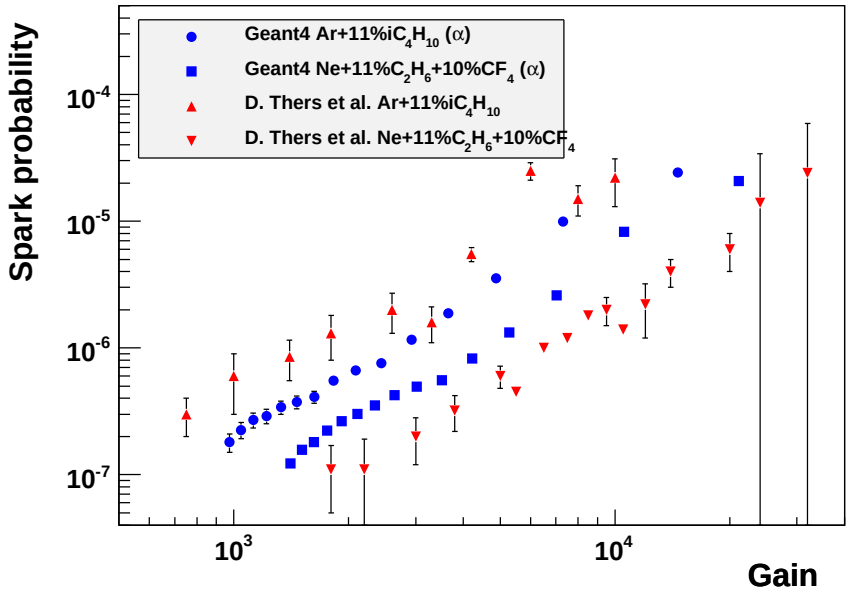

Figure 10: Comparison between measured and simulated spark rate as a function of the gain for argon and neon mixtures. Data are extracted from the Figure 8 in [3].

6 Comparison between a standard and a bulk (woven mesh) Micromegas

The fact that a non negligible part of the HIPs are produced on the micro-mesh may be problematic in the case of a bulk Micromegas, where the woven mesh used is much

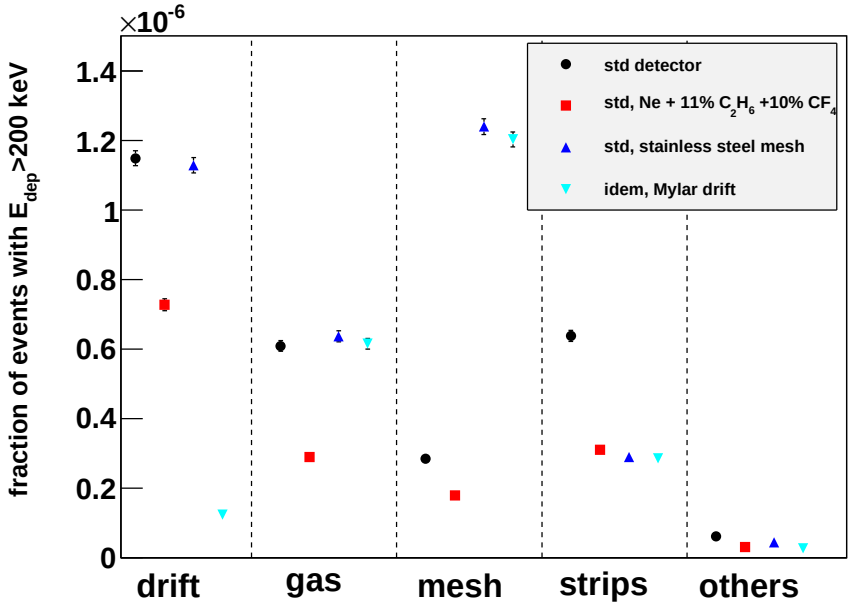

Figure 11: Contribution of the different parts of the detector to the production of energy deposits larger than 200 keV for various geometries.

thicker (30 microns of stainless steel) than meshes of standard Micromegas (4 microns of nickel). We therefore investigated the importance of the material and thickness of the micro-mesh. The results are shown in Figure 12 and indicate that the effect of the micro-mesh is relatively small. In particular, we predict that the bulk Micromegas should not spark significantly more than Micromegas equipped with thin nickel mesh. This is due to a partial compensation between HIPs coming from the mesh and the strips. Indeed, a thicker mesh will produce more HIPs, but will also absorb more HIPs coming back from the strips. This effect is illustrated in Figure 11, where we see a decrease of the strip contribution by a factor of two.

7 Experimental tests to check our simulation

We now propose a few experimental tests that would help to check the validity of our interpretation. As mentioned before, the comparison of the spark rate between standard and bulk Micromegas would be a very good test. Another simple check would be to tilt the detector with respect to the beam axis. The beam particles would therefore cross more material in the detector, leading to a higher spark rate, as illustrating in Figure 13.

However, these predictions could not help to determine the contributions of the HIPs produced through interactions with the gas or with the drift electrode of the detector. A test that would unambiguously check our interpretation would be to use two identi-

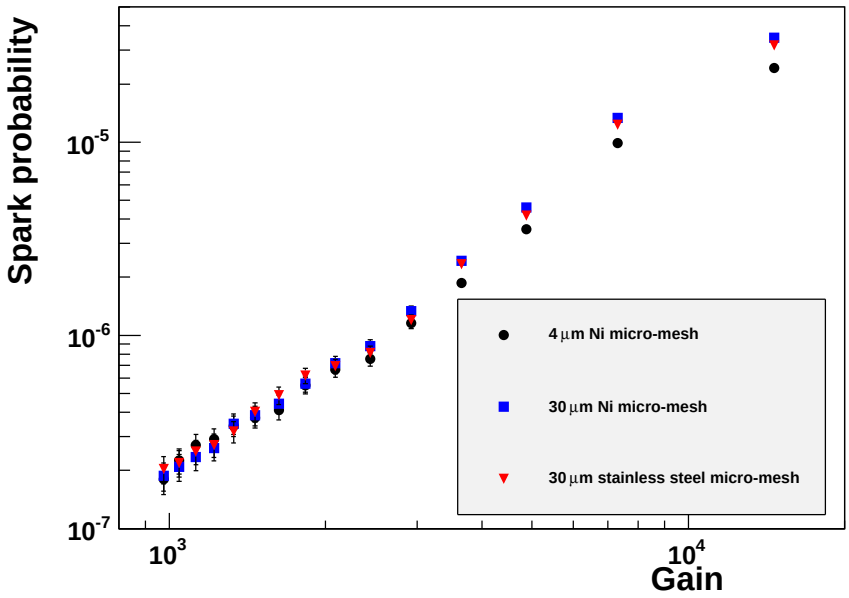

Figure 12: Simulated spark rate for different types of micro-mesh, with an argon-isobutane mixture (89-11).

cal detectors, one equipped with an aluminized mylar for the drift electrode, and one equipped with a thick, woven mesh. As shown in Figure 14 a significantly smaller spark rate is expected with the first detector. Figure 11 indicates that an aluminized mylar can decrease the contribution of the drift electrode by roughly an order of magnitude.
Tests have been performed recently at CERN within the RD51 collaboration, using a 150 GeV pion beam, with standard and bulk Micromegas, as well as with different types of drift electrodes. These tests were primarily performed to measure the spark rate in a transverse magnetic field, and study the dependence with the Lorentz angle [12], but the analysis of the data taken will also allow us to check our predictions.

8 Conclusion

We presented a Geant4-based study of the origin of the sparks in a Micromegas detector hit by hadron beams. Highly ionizing particles are produced by nuclear interactions of hadrons with the drift electrode, the gas, the micro-mesh and the strips of the detector. Within this interpretation, we were able to explain qualitatively the two main observations obtained with hadron beams: i) the gain dependence of the spark rate, and ii) the strong effect of the gas mixture, that seems to come essentially from stopping power differences. Using a gain normalization from sparks with an alpha source, our simulation gives a correct

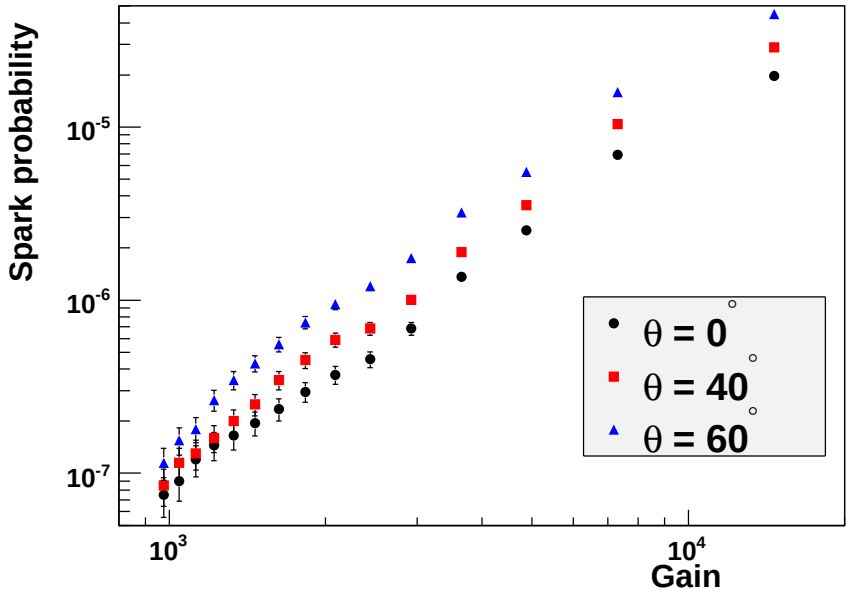

Figure 13: Simulated spark rate for different crossing angles of 15 GeV pion beams, with an argon-isobutane mixture (89-11).

estimate of the spark rate in hadron beams. Several tests were proposed to experimentally confirm this interpretation, namely the spark rate dependence with the incident angle of beam particles, the increase of the spark rate by using a thick mesh for the drift electrode (instead of an aluminized mylar), or the spark rate comparison between a standard and a bulk Micromegas.

9 Acknowledgments

We would like to thank A. Boudard, M. Garçon, I. Giomataris, P. Kaitaniemi, F. Kunne, A. Magnon, D. Neyret and D. Thers for many fruitful discussions. Special thanks are also due to M. Ungaro for his patient help on Gemc. This work was funded by French Agence Nationale pour la Recherche Contract no. ANR-07-BLAN-0338.

References

[1] Y. Giomataris *et al.*, Nucl. Instrum. Methods A **376** (1996) 29

[2] H. Raether, Z. Phys. **112** (1939) 464

[3] D. Thers *et al.*, Nucl. Instrum. Methods A **469** (2001) 133

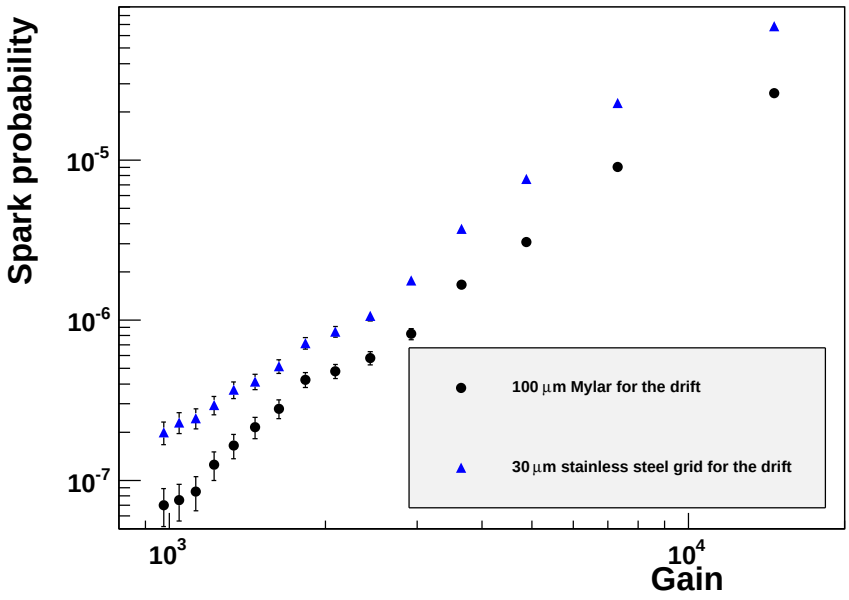

Figure 14: Comparison of the simulated spark rate with 15 GeV pions, using an aluminized mylar or a stainless steel mesh for the drift electrode, with an argon-isobutane mixture (89-11).

[4] A. Bay *et al.*, Nucl. Instrum. Methods A **488** (2002) 162

[5] Geant4 - a simulation toolkit, Nucl. Instrum. Methods A **506** (2003) 250

[6] M. Ungaro, GEant4 Monte Carlo, http://clasweb.jlab.org/wiki/index.php/CLAS12_Softwa

[7] http://www.geant4.org/geant4/support/proc_mod_catalog/physics_lists/useCases.shtml

[8] see http://geant4.cern.ch/support/proc_mod_catalog/models/hadronic/ for QGSP, QGSC, Bertini and Binary

[9] S. Banerjee, CHEP 2009, http://geant4.cern.ch/results/talks/CHEP09/CHEP09-validatio

[10] G. Puill, *Le développement de Micromegas, un nouveau détecteur gazeux de position à microgrille*, PhD (June 2000), http://cdsweb.cern.ch/record/466540/files/

[11] CRC Handbook of Chemistry and Physics, 89^{th} Edition, 2008-2009, 15-43

[12] P. Konczykowski *et al.*, Nucl. Instrum. Methods A (2009), doi:10.1016/j.nima.2009.10.105